Talanta 119 (2014) 632–638

Contents lists available at ScienceDirect

Talanta

journal homepage: www.elsevier.com/locate/talanta

Two hexaazatriphenylene based selective off–on fluorescent chemsensors for cadmium(II)

Xiao-Hong Zhang [a,b], Chuan-Fang Zhao [a,b], Yue Li [a,b,*], Xiu-Ming Liu [a,b], Ao Yu [a,b], Wen-Juan Ruan [a,b,*], Xian-He Bu [a,b]

[a] Department of Chemistry, Nankai University, Tianjin 300071, PR China
[b] Tianjin Key Laboratory on Metal and Molecule-Based Material Chemistry, Nankai University, Tianjin 300071, PR China

ARTICLE INFO

Article history:
Received 26 June 2013
Received in revised form
21 October 2013
Accepted 1 November 2013
Available online 20 November 2013

Keywords:
Hexaazatriphenylene
Off–On
Chemsensor
Cd^{2+} ion

ABSTRACT

Two hexaazatriphenylene (HAT) derivatives, 2,3,6,7-tetramethyl-10,11-di(pyridin-2-yl)dipyrazino[2,3-f:2',3'-h]quinoxaline (**1**) and 2,3-dimethyl-6,7,10,11-tetra(pyridin-2-yl)dipyrazino[2,3-f:2',3'-h]quinoxaline (**2**), were designed and synthesized. Both **1** and **2** exhibited high off–on fluorescent selectivity for Cd^{2+} over many other metal ions, and the detection limits were determined to be 0.6 and 5.0 μM, respectively. The stoichiometry and coordination mode of blue fluorescent **1**-Cd^{2+} and cyan fluorescent **2**-Cd^{2+} were determined with fluorescence titration fit, Job's plot analysis, ^1H NMR titration and X-ray crystallography, and the fluorescence enhancement mechanism was analyzed with density functional theory calculation.

1. Introduction

Cadmium (Cd), which is widely used in industry, agriculture and many other fields, has caused serious environmental problems [1–3]. It is recognized that Cd is a highly toxic element and is easy to be absorbed and accumulated by plants and animals to the levels dangerous to their health [4–6]. Excessive exposure to Cd^{2+} would cause serious health disorders even certain cancer. It is in great need for the development of methods to detect and monitor Cd level. Due to the operability and sensitivity, fluorescent sensors are powerful tools for the detection of metal ions and widely used not only in environmental monitoring but also in biological studies [7–11]. In recent years, a large number of fluorescent sensors have been reported for the detection of Cd^{2+} ion [12–15]. However, because of the similar chemical properties of Cd^{2+} and Zn^{2+}, most of these sensors also respond to Zn^{2+} ion [16–19]. Hence, it is still a great challenge to develop Cd^{2+} selective sensors that are immune to the interference of Zn^{2+} and other metal ions [20,21].

The general basis of designing a molecular sensor for selective recognition is the host–guest interaction, such as hydrogen bonding, electrostatic force, metal–ligand coordination, hydrophobic interaction and van der Waals interaction [22–24]. The challenge in developing fluorescent sensors is to enhance the induced signal of a particular target [25–27]. Conjugated aromatic structures, which are characterized with extensive π-electron delocalization and strong fluorescent emission, have been widely used as fluorophores in amplified chemosensory systems [28–30]. In recent years, π-conjugated hexaazatriphenylene (HAT) derivatives, which are obtained from the modification of HAT core (Chart 1) with various substituent groups, have received intense attention because of their applications in n-type semiconductor [31,32], liquid crystal [33,34], magnetic material [35,36] and coordinate self-assembly [37–39]. The application of HAT derivatives in fluorescent chemsensor was also attempted in recent years [40]. Although some positive results have been reported, the research in this area is still at the initial stage. In our previous work, we have developed two phenyl substituted HAT derivatives for the detection of Zn^{2+} [41]. Considering that Cd^{2+} has similar electronic structure but larger size relative to Zn^{2+}, we assume that replacing the phenyls with smaller substituents, such as methyl, which would reduce the steric hindrance to metal ions and thus enhance the binding ability to Cd^{2+}, is a promising strategy for the design of Cd^{2+} response fluorescent sensors.

In this work, two methyl substituted HAT derivatives, 2,3,6,7-tetramethyl-10,11-di(pyridin-2-yl)dipyrazino[2,3-f:2',3'-h]quinoxaline (**1**) and 2,3-dimethyl-6,7,10,11-tetra(pyridin-2-yl)dipyrazino[2,3-f:2',3'-h]quinoxaline (**2**), were designed and synthesized conveniently by two step reactions (see Scheme 1). They both exhibit selective turn-on fluorescent recognition of Cd^{2+} ion that is nearly unaffected by many other background metal ions including Na^+, K^+,

* Corresponding authors at: Department of Chemistry, Nankai University, No. 94 of Weijin Road, Tianjin 300071, PR China. Tel.: +86 22 23501717; fax: +86 22 23502458.
E-mail addresses: liyue84@nankai.edu.cn (Y. Li), wjruan@nankai.edu.cn (W.-J. Ruan).

0039-9140/$ - see front matter © 2013 Elsevier B.V. All rights reserved.
http://dx.doi.org/10.1016/j.talanta.2013.11.009

Ca^{2+}, Mg^{2+}, Mn^{2+}, Fe^{2+}, Co^{2+}, Ni^{2+}, Cu^{2+}, Zn^{2+}, Ag^{+} and Pb^{2+}. The recognition behaviors of **1** and **2** to Cd^{2+} ion were investigated by fluorescence titration, UV–vis spectrum, ^1H NMR titration and the single X-ray crystallographic method. Time-dependent density functional theory (TD-DFT) calculation was further carried out to explore the mechanism of fluorescent enhancement of **1** and **2** upon coordination with Cd^{2+}.

2. Experimental

2.1. Materials and general methods

All reagents and chemicals were obtained commercially and used as received unless stated otherwise. All solvents used for photophysical studies were purified by standard procedures. The ^1H NMR spectrum was measured in $CDCl_3$ with a Bruker 400 MHz NMR spectrometer with chemical shifts reported as ppm. Elemental analyses (C, H, and N) were tested using a Perkin-Elmer 240C analyzer. IR spectra were recorded on a TENSOR 27 OPUS Fourier transform infrared (FT-IR) spectrometer (Bruker) using KBr disks dispersed with sample powders in the 4000–400 cm^{-1} range. UV–vis absorption spectra were measured on a Shimadzu UV-2450 spectrophotometer and fluorescence spectra were recorded on a Varian Cary Eclipse fluorescence spectrometer. Mass spectra were detected in a TRACE DSQ spectrometer.

2.2. Preparation of solutions for fluorescence and absorption

Solutions of metal ions (K^{+}, Na^{+}, Ca^{2+}, Mg^{2+}, Mn^{2+}, Fe^{2+}, Co^{2+}, Ni^{2+}, Cu^{2+}, Ag^{+}, Pb^{2+}, Zn^{2+} and Cd^{2+}) of 0.03 M in acetonitrile were prepared. The concentration of **1** in the fluorescence and UV–vis titration experiments was 50 μM with acetonitrile as solvent, and that of **2** was 10 μM. For all of the fluorescent measurements, the excitation wavelength was 320 nm with excitation and emission slit widths of 5 nm at room temperature.

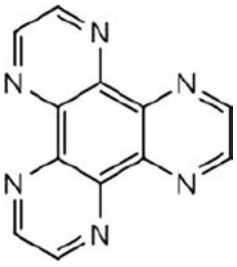

Chart 1. The structure of HAT .

2.3. Synthesis of 2,3,6,7-tetramethyl-10,11-di(pyridin-2-yl) dipyrazino[2,3-f:2′,3′-h]quinoxaline (1)

The synthetic routes of the target HAT derivatives are outlined in Scheme 1. Hexaaminobenzene (HAB) was prepared according to the literature method [42,43]. Under nitrogen atmosphere, HAB (1.3 g, 7.7 mmol) was dissolved in a mixture of water (75 mL) and ethanol (220 mL), and the solution was heated to 50 °C in 10 min. Then a solution of 2,3-butanedione (1.3 g, 15.4 mmol) in ethanol (70 mL) was added dropwise. The reaction mixture was stirred for 2 h and then allowed to cool down to room temperature. The solid product diamine (**3**) was filtered, washed with ethanol and used directly in the next reaction steps. Under nitrogen atmosphere, 2,2-pyridil (318 mg, 1.5 mmol) and **3** (268 mg, 1 mmol) were added to the mixture of ethanol (30 mL) and acetic acid (0.5 mL) and refluxed for 3 h. The reacted solution was filtered and further purified by column chromatography (silica gel) using chloroform/methanol (30/1) as eluent to collect the main fraction. After removing solvent, white target product was obtained in yield of 21%. ^1H NMR (300 MHz, $CDCl_3$) δ 8.41 (d, J=4.2 Hz, 2H), 8.19 (d, J=7.8 Hz, 2H), 7.86 (td, J=7.7, 1.7 Hz, 2H), 7.28 (ddd, J=7.6, 4.9, 1.1 Hz, 2H), 2.98 (d, J=4.8 Hz, 12H). MS (ESI-MS) m/z: 445.6 $[M+H]^+$. Anal. Calcd. for $C_{28}H_{22}N_6 \cdot H_2O$: C, 67.52; H, 5.00; N, 24.30%; Found: C, 67.26; H, 4.79; N, 24.23%. IR (KBr, cm^{-1}): 1650, 1587, 1383, 1245, 743.

2.4. Synthesis of 2,3-dimethyl-6,7,10,11-tetra(pyridin-2-yl) dipyrazino[2,3-f:2′,3′-h]quinoxaline (2)

Compound **2** was prepared via a similar procedure to that of **1**. A white solid was obtained with yield of 24%. ^1H NMR (300 MHz, $CDCl_3$) δ 8.46–8.28 (m, 8H), 7.95 (t, J=7.6 Hz, 4H), 7.35–7.25 (m, 4H), 3.00 (s, 6H). MS (ESI-MS) m/z: 633.6 $[M+Na+K+H]^+$. Anal. Calcd. for $C_{46}H_{28}N_8 \cdot 2H_2O$: C, 57.14; H, 5.36; N, 19.60%; Found: C, 57.47; H, 5.21; N,19.02%. IR (KBr, cm^{-1}): 1587, 1472, 1369, 1374, 1220, 998, 792, 744, 595.

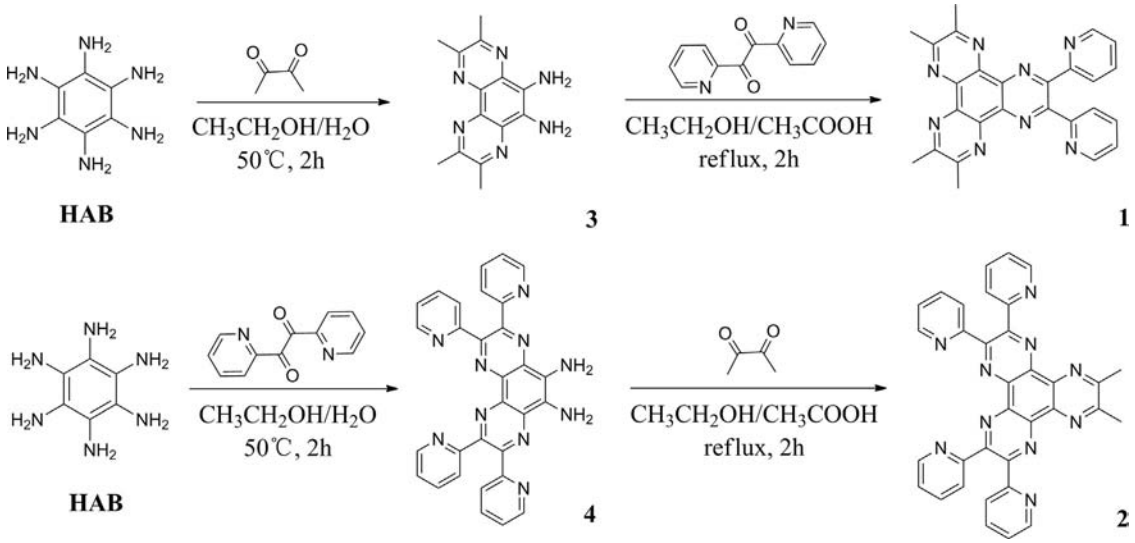

Scheme 1. Synthetic routes of **1** and **2**.

2.5. Synthesis of the single crystals of **1**-Cd and **2**-Cd

Compound **1** (0.01 mmol) and $CdCl_2$ (0.05 mmol) were dissolved in dichloromethane/methanol (3 mL, $v/v=1/2$), the mixture was sealed in a small capped vial and heated at 95 °C for 3 days, followed by slow cooling to room temperature in 12 h. Yellow crystals of **1**-Cd were collected. Single crystals of **2**-Cd suitable for X-ray analysis were obtained by a similar method to **1**-Cd. Compound **2** (0.01 mmol) and $Cd(NO_3)_2\cdot 4H_2O$ (0.05 mmol) were dissolved in dichloromethane/methanol (3 mL, $v/v=1/2$), the mixture was sealed in a small capped vial and heated at 65 °C for 3 days, followed by slow cooling to room temperature in 12 h. The crystals of **2**-Cd were also bright yellow. CCDC reference nos. are 922743 and 920384 for **1**-Cd and **2**-Cd, respectively.

2.6. X-ray data collection and structure determinations

X-ray single-crystal diffraction data for complexes **1**-Cd and **2**-Cd were collected on a SuperNova, Dual, Cu at zero, Atlas diffractometer at 100.01(10) K with Mo-Kα radiation ($\lambda=0.71073$ Å) by ω scan mode. The program SAINT [44] was used for integration of the diffraction profiles. All the structures were solved by direct methods using the SHELXS program of the SHELXTL package and refined with SHELXL (semi-empirical absorption corrections were applied using SADABS program) [45]. The final refinement was performed by full matrix least-squares methods with anisotropic thermal parameters for non-hydrogen atoms on F^2. The hydrogen atoms of the ligands were generated theoretically onto the specific atoms and refined isotropically with fixed thermal factors. The electron density of the disordered guest molecules in complex **1**-Cd was treated using the SQUEEZE routine of PLATON [46–49]. The results were appended to the bottom of the CIF file. The number of located electrons is 74 per unit cell, which is included in the formula, formula weight, calculated density, and F(000). These residual electron densities are assigned to one molecule of methanol. So SQUEEZE one methanol molecule per formula unit. This value calculated based upon electrons analysis (One methanol molecule would give 18e.). So the tentative formula for this compound is presented in the text as $Cd_3C_{28}H_{28}N_8O_2Cl_6$. Detailed crystallographic data (after the SQUEEZE) are summarized in Tables S1 and S2.

2.7. Theoretical calculations

Theoretical investigations on **1**, **2** and their complexes with Cd^{2+} were performed by the Gaussian09 program package [50]. The geometries of ligands and complexes were completely optimized by the B3LYP exchange-correlation functional [51–54] with LANL2DZ [55] basis set and pseudopotential applied to Cd^{2+} ions and 6–31G(d) applied to the atoms of ligands. All the final structures were confirmed by frequency calculation to be the real minima without any imaginary frequency. Based on the optimized structures, the excitation properties of these compounds were calculated with the TD-DFT method at the same level.

3. Results and discussion

3.1. Fluorescence studies

The fluorescence response of compounds **1** and **2** was investigated in acetonitrile with the excitation at 320 nm. Free compound **1** (50 μM) exhibited a weak emission with the maximum at 391 nm and extremely low fluorescence quantum yield of 0.002 (Fig. 1a). Upon the addition of Cd^{2+} ion, a pronounced fluorescence peak at 438 nm appeared. The emission intensity increased by 72-fold ($I_{438}^{\mathbf{1\text{-}Cd}}/I_{391}^{\mathbf{1}}$), and the quantum yield increased by

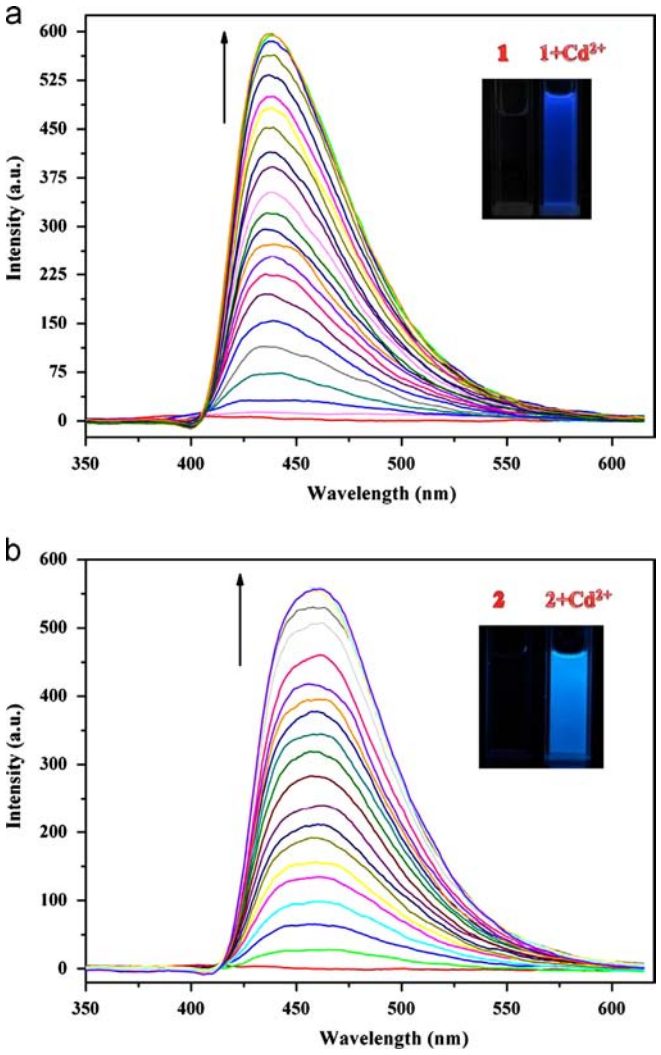

Fig. 1. (a) Fluorescence emission spectra of **1** (50 μM) in acetonitrile upon the addition of Cd^{2+} from 0 to 5 mM. (b) Fluorescence emission spectra of **2** (10 μM) in acetonitrile upon the addition of Cd^{2+} from 0 to 2.2 mM. The excitation and emission slit widths were 5 nm and λ_{ex} was 320 nm. Color changes (left) and fluorescence changes excited by UV lamp (365 nm) (right) in compounds **1** (a) and **2** (b) upon addition of Zn^{2+}.

20-fold. Accordingly, under the irradiation of an UV lamp (centered at 365 nm), the solution of **1** changed from non-luminous to blue fluorescent upon the addition of Cd^{2+}, which could be observed directly by naked eyes (Fig. 1a insert). The fluorescence response of compound **2** to Cd^{2+} ion was analogous to that of **1** (Fig. 1b). With the addition of Cd^{2+} ion to **2** solution (10 μM), a new strong emission band with the maximum at 457 nm appeared and the fluorescence quantum yield increased from 0.004 to 0.06. The fluorescent color of the solution of **2** changed from dark to cyan with Cd^{2+} addition (irradiated with UV lamp, Fig. 1b insert). Apparently, both **1** and **2** have off–on response to Cd^{2+} ion.

The sensitivities of compounds **1** and **2** toward Cd^{2+} were examined with fluorescence titration experiments (also shown in Fig. 1). The emission spectra of a batch of their solutions (50 μM for **1** and 10 μM for **2**) with gradually increased addition amount of Cd^{2+} were recorded. It was observed that, for both **1** and **2**, the intensity of the fluorescent emission band enhanced drastically with the analytic amount in the low concentration range and leveled off at high concentration to saturation. At low Cd^{2+} concentrations (0–110 μM for **1** and 0—550 μM for **2**), a good linear correlation ($R^2=0.993$ for **1** and 0.992 for **2**) exists between the fluorescence enhancement extent and the addition amount of

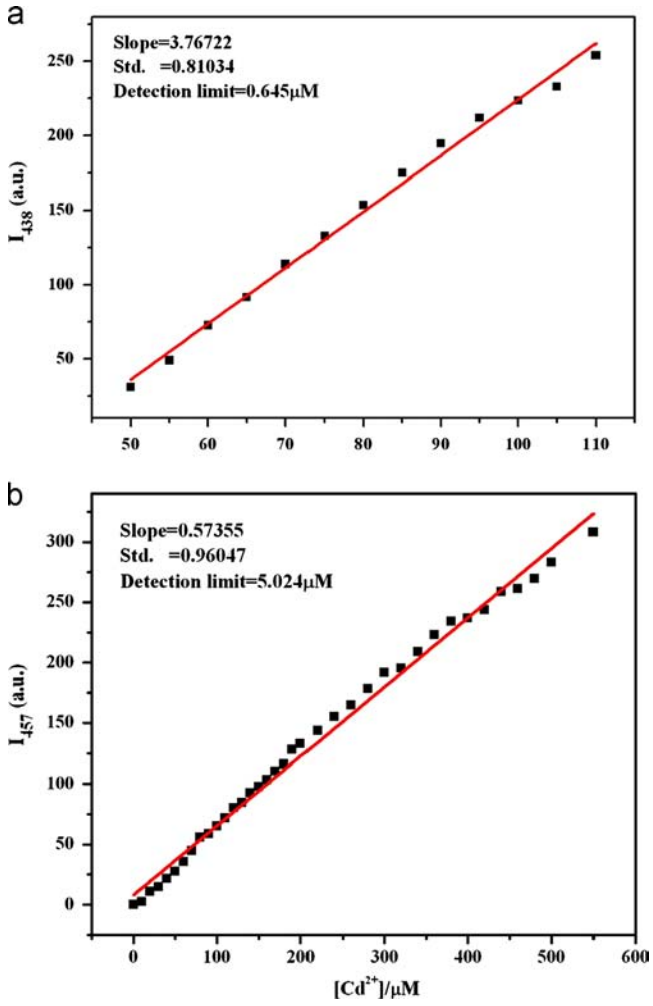

Fig. 2. Linear emission intensity change of **1** (a) and **2** (b) as a function of the concentration of Cd^{2+} ion.

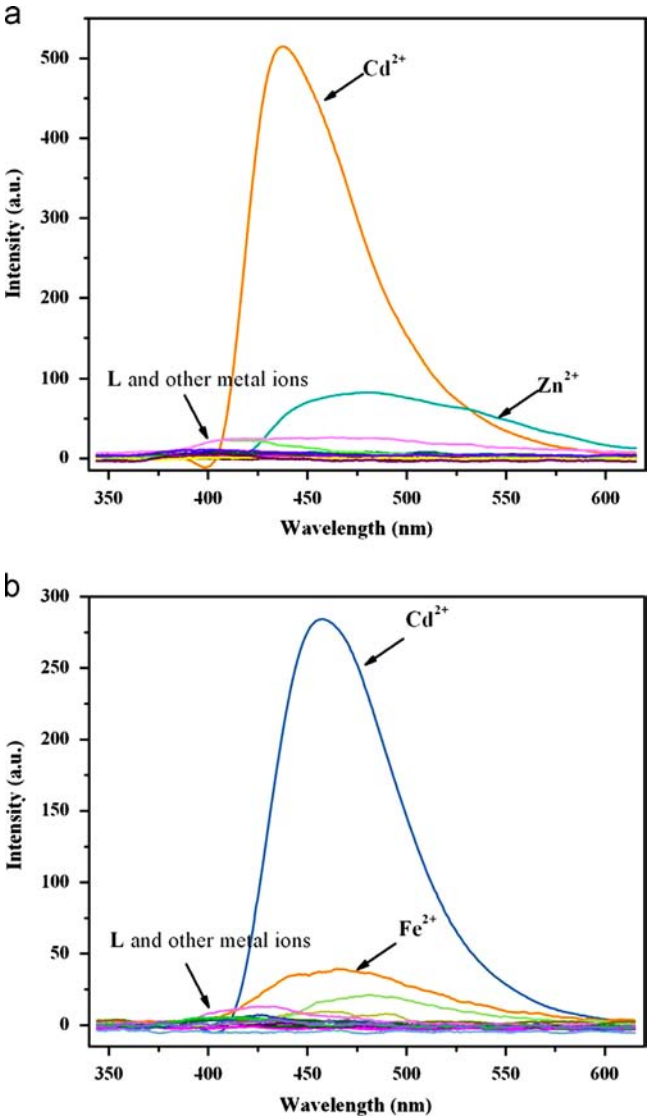

Fig. 3. Fluorescence emission spectra (λ_{ex}=320 nm) of (a) **1** (50 μM) and (b) **2** (10 μM) in the presence of different metal ions (10 equiv for 1 and 50 equiv for 2) in acetonitrile. The excitation and emission slit widths were 5 nm.

Cd^{2+} (Fig. 2). From the slopes of the fitting lines of the data in the linear response range (k) and the deviation of fluorescent measurements (σ), the detection limits of **1** and **2** towards Cd^{2+} ($3\sigma/k$) were calculated to be 0.6 and 5.0 μM, respectively. The detection limit of **1** is lower than that of **2**, which means that **1** is more sensitive to Cd^{2+} relative to **2** and may result from the different binding modes of **1**-Cd^{2+} and **2**-Cd^{2+}.

The fluorescence titration experiments also provide information about the binding modes and stability of **1** and **2** to Cd^{2+} ion. The nonlinear fit of the titration data shows that **1** coordinates to Cd^{2+} in 1:2 stoichiometry and the logarithm of the cumulative stability constant ($\log\beta$) is 9.1, while **2**-Cd^{2+} presents the stoichiometry of 1:3 and the $\log\beta$ of 10.1 (Fig. S1) [56,57]. Job's plot analysis also supported the 1:2 stoichiometry of **1**-Cd^{2+} and 1:3 stoichiometry of **2**-Cd^{2+} (Fig. S2). The difference in the binding stoichiometry between **1**-Cd^{2+} and **2**-Cd^{2+} is mainly due to the distinct binding sites of **1** and **2**, that is, **1** has two chelate sites but **2** possesses three.

3.2. Selection and competition experiments

Since the response specifity is essential for a chemsensor, we also tested the fluorescent response of these two compounds to other common metal ions. As shown in Fig. 3, in contrast to Cd^{2+}, the addition of excess Na^{+}, K^{+}, Mg^{2+}, Ca^{2+}, Mn^{2+}, Fe^{2+}, Co^{2+}, Ni^{2+}, Cu^{2+}, Zn^{2+}, Ag^{+}, and Pb^{2+} to the solution of **1** (50 μM) and **2** (10 μM) only caused negligible change in the fluorescence emission, which shows that these two compounds have excellent selectivity to Cd^{2+} over other metal ions. We further investigated the fluorescence selectivity of **1** and **2** in the mixed solvent of acetonitrile and water. Both **1** and **2** can maintain the superior selectivity to Cd^{2+} until water content was raised to 5% (Fig. S3).

Another important criterion for a selective sensor is its ability to detect a specific species under the interference of other competing ions. To further assess the Cd^{2+}-selectivity of **1** and **2**, competition experiments were conducted by the addition of Cd^{2+} ion to the solution of **1** or **2** coexistent with other metal ions. As shown in Fig. 4, the emission intensity of **1**-Cd^{2+} was nearly unperturbed in the presence of other metal ions except Ni^{2+} and Cu^{2+}. Similarly, compound **2** also displays good recognition of Cd^{2+} over other metal ions except Ni^{2+} and Cu^{2+}. These results mean that compounds **1** and **2** have a higher affinity with Cd^{2+}.

It is well known that, because of the similar chemical properties between Zn^{2+} and Cd^{2+}, the discrimination of these two metal ions is very difficult. However, in this work, the fluorescent emission of **1**-Zn^{2+} and **2**-Zn^{2+} enhanced remarkably upon the addition of Cd^{2+}, that is, I/I_0 increased from 1.4 to 56.2 for **1**-Zn^{2+}, and from 7.5 to 156.9 for **2**-Zn^{2+}(measured respectively at 438 and 457 nm, Fig. S4). These results prove that both **1** and **2** can easily

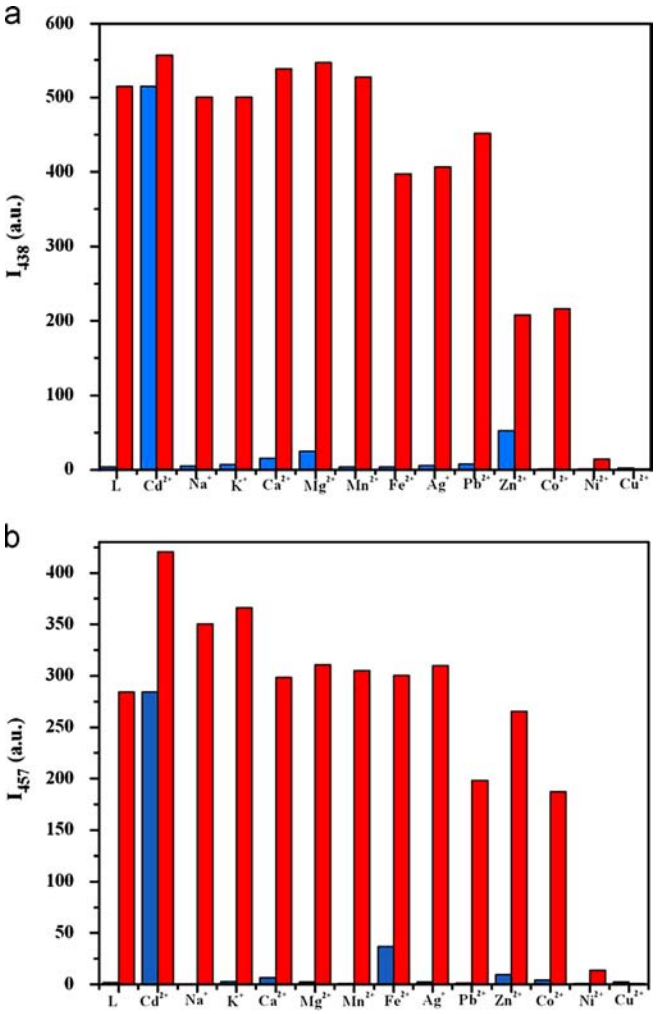

Fig. 4. Competitive selectivity of **1** (a) and **2** (b) towards Cd^{2+} in the presence of different metal ions in acetonitrile. Excitation at 320 nm. Bars represent the final fluorescence intensity at 438 nm for **1** or 457 nm for **2**. Blue bars represent the addition of 10 equiv of metal ions to a solution of **1** (50 μM) or 50 equiv of metal ions to **2** (10 μM). Red bars represent the subsequent addition of 10 equiv of Cd^{2+} to the solution of **1** or 50 equiv of Cd^{2+} to **2**.

distinguish Cd^{2+} from Zn^{2+}, and the fluorescent response of **2** to Cd^{2+} is absolutely free from the interference of Zn^{2+}.

3.3. UV–vis titration

Further investigation was carried out on the changes of UV–vis spectra upon the addition of Cd^{2+} ion to **1** (50 μM) and **2** (10 μM) in acetonitrile (Fig. 4). The absorption spectrum of **1** exhibited two bands at 281 and 315 nm. With the increase of Cd^{2+} addition amount, the absorption at 281 nm gradually decreased, and a new red-shift band at 292 nm appeared simultaneously with three isosbestic points at 297, 306 and 330 nm, which indicates the formation of a new species from **1** and Cd^{2+}. For **2**, the absorption peak at 293 nm red-shifted to 309 nm with isosbestic points at 299, 324 and 350 nm. We assume that the changes in the UV–vis absorption mainly arise from the coordination of Cd^{2+} ions with the N atoms of ligands **1** or **2**, which enhances the planarity of the ligands.

3.4. ^1H NMR titration study

To understand the nature of the interaction between sensors and Cd^{2+}, ^1H NMR titrations in $CDCl_3$–CD_3CN (1:2) were carried out. For compound **1** (Fig. S5a), upon the addition of Cd^{2+}, the signals of H^1 downfield shifted from 8.36 to 9.10. Moreover, H^5 of the methyl group downfield shifted by 0.17 ppm, while H^6 of another methyl group just moved by 0.05 ppm. The changes of the signals of H^1, H^5 and H^6 indicate the coordination of Cd^{2+} with N^1–N^6. The addition of 1 equiv Cd^{2+} made the H signals of **1** broaden. After the addition of 2 equiv Cd^{2+}, well-separated peaks were obtained, suggesting the formation of a stable complex [58,59]. No shift in the position of proton signals was observed with further addition of Cd^{2+}, which confirms the 1:2 binding mode of **1**-Cd^{2+}.Fig. 5

For compound **2** (Fig. S5b), the signals of H^1 and $H^{1'}$ split into two peaks and moved from 8.37 to 9.05 and 9.15, respectively. Similar phenomenon was observed in H^4 and $H^{4'}$, which suggests the binding of Cd^{2+} with all the N atoms. After the addition of 3 equiv Cd^{2+} ion, well-separated peaks appeared, which supports the 1:3 stoichiometry of **2**-Cd^{2+}.

3.5. Crystal structure

The crystal structures of **1**-Cd and **2**-Cd are shown in Figs. 6, S6 and S7. The crystallographic data and relevant refinement

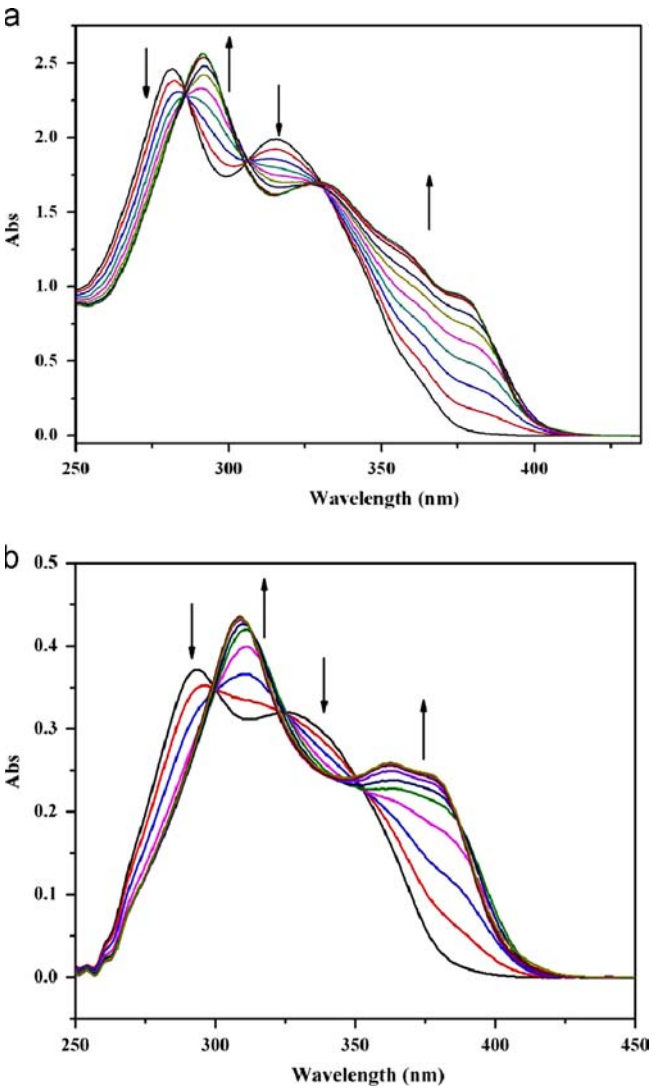

Fig. 5. (a) Absorption spectra of **1** (50 μM) in acetonitrile upon the addition of Cd^{2+} from 0 to 50 μM. (b) Absorption spectra of **2** (10 μM) in acetonitrile upon the addition of Cd^{2+} from 0 to 10 μM.

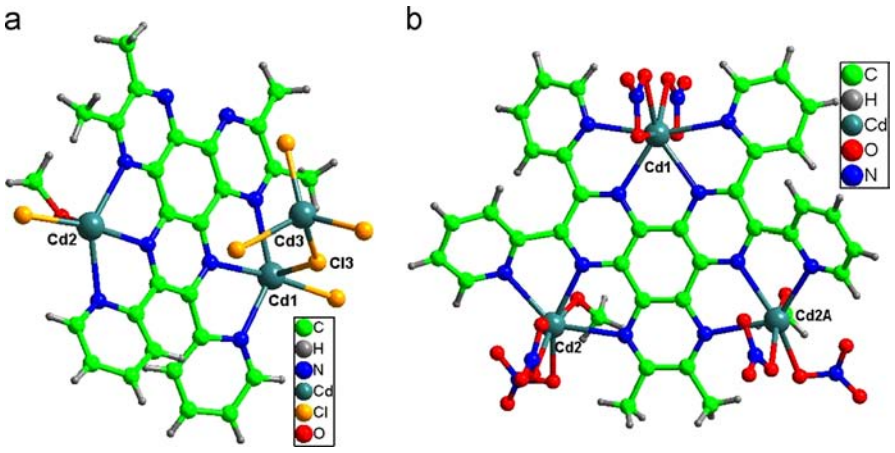

Fig. 6. Crystal structures of **1**-Cd (a) and **2**-Cd (b).

parameters are tabulated in Table S1, and the selected bond lengths and bond angles are listed in Table S2.

As shown in Fig. 6a, even though three Cd^{2+} ions are contained in the asymmetric unit of **1**-Cd, **1** coordinates directly only to Cd1 and Cd2, while Cd3 is linked with Cd1 via bridging Cl3. In complex **2**-Cd, one ligand **2** chelates three Cd^{2+} ions through 10 N atoms (Fig. 6b). These results confirm the 1:2 stoichiometry of **1**-Cd^{2+} and 1:3 stoichiometry of **2**-Cd^{2+} obtained from fluorescence titration, Job's plot analysis and ^{1}H NMR titration (discussed above).

In free **1** and **2** molecules, the rotation of the C–C bonds between pyridine rings and HAT core would cause the nonradiative relaxation of the excitation state. The chelation to Cd^{2+} would restrict the rotation of these C–C bonds, and thus enhance the fluorescent emission. Additionally, the enhancement of the molecular coplanarity would extend the conjugate system and thus lower the π–π^* energy gap, which explains the red-shift observed in the UV–vis spectrum.

3.6. Theoretical studies

TDDFT calculation was carried out to analyze the enhancement effect of Cd^{2+} on the fluorescence emission of **1** and **2**. As shown in Fig. S8, for all the ligands and complexes, the calculated UV–vis spectra match well with the experimental spectra. The consistence between calculated and experimental spectra proves the reliability of our calculation. The error of our calculation may be caused by the solvent effect and Stoke's shift.

TDDFT calculation suggests that, for **1**-Cd^{2+}, the bands with lower energy ($400\ nm < \lambda < 480\ nm$) should be assigned to the transitions from HOMO, HOMO−1, HOMO−2 and HOMO−3 to LUMO, LUMO+1 and LUMO+2 (Table S3). The scrutinizing of the structures of these orbitals shows that HOMO–HOMO−3 mainly locate on ligand **1**, while LUMO–LUMO+2 distribute primarily around Cd atom (Fig. S9), that is, the excitations between these orbitals involve the charge transfer from ligand to metal. In contrast, the low energy bands ($400\ nm < \lambda < 530\ nm$) of **2**-$Cd^{2+}$ mainly involve the transitions from HOMO–HOMO−3 to LUMO, LUMO+3 and LUMO+4 (Table S4). All these orbitals distribute on the ligand (Fig. S10), which means that these transitions are $\pi \rightarrow \pi^*$ in nature. Therefore, the fluorescent emission of **2**-Cd^{2+} at 457 nm originates from the π^* excited state of the ligand.

4. Conclusions

We have successfully synthesized two new HAT based off–on fluorescent sensors (**1** and **2**), which are selective for Cd^{2+} over many other metal ions. Upon formation of a 1:2 complex with Cd^{2+} ion, the fluorescent color of **1** turns from dark to blue, while a 1:3 stoichiometric complex between **2** and Cd^{2+} ion is formed with fluorescent color change from dark to cyan. Both the fluorescence emission enhancements of **1**-Cd^{2+} and **2**-Cd^{2+} could be explained with the chelation enhanced fluorescence (CHEF) effect [60–62], which is fully supported by their crystal structures and further analyzed by the DFT calculation. These results show that HAT derivatives have potential application in fluorescence sensor. Further studies are in progress in our laboratory.

Acknowledgments

This work was supported by the 973 Program (2012CB821700), and NSFC (21031002 and 51073079).

Appendix A. Supplementary materials

Supplementary materials associated with this article can be found in the online version at http://dx.doi.org/10.1016/j.talanta.2013.11.009.

References

[1] L. Pari, P. Murugavel, S.L. Sitasawad, K.S. Kumar, Life Sci. 80 (2007) 650–658.
[2] Lyn Patrick, N.D. Altern, Med. Rev. 8 (2003) 106–128.
[3] R.L. Chaney, J.A. Ryan, Y.M. Li, S.L. Brown, in: M.J. McLaughlin, B.R. Singh (Eds.), In Cadmium in Soils and Plants, Kluwer, Boston, 1999, pp. 219–256.
[4] C.C. Bridges, R.K. Zalups, Toxicol. Appl. Pharmacol. 204 (2005) 274–308.
[5] M. Waisberg, P. Joseph, B. Hale, D. Beyersmann, Toxicology 192 (2003) 95–117.
[6] R.K. Zalups, S. Ahmad, Toxicol. Appl. Pharmacol. 186 (2003) 163–188.
[7] D.A. Safin, M.G. Babashkina, Y. Garcia, Dalton Trans. 42 (2013) 1969–1972.
[8] H.R. Li, W.J. Cheng, Y. Wang, B.Y. Liu, W.J. Zhang, H.J. Zhang, Chem. Eur. J. 16 (2010) 2125–2130.
[9] E. Tamanini, A. Katewa, L.M. Sedger, M.H. Todd, M.F. Watkinson, Inorg. Chem. 48 (2009) 319–324.
[10] K. Komatsu, Y. Urano, H. Kojima, T.J. Nagano, J. Am. Chem. Soc. 129 (2007) 13447–13454.
[11] Z.H. Lin, S.J. Ou, C.Y. Duan, B.G. Zhang, Z.P. Bai, Chem. Commun. (2006) 624–626.
[12] W. Wang, Q. Wen, Y. Zhang, X. Fei, Y. Li, Q. Yang, X. Xu, Dalton Trans. 42 (2013) 1827–1833.
[13] Y. Liu, X. Dong, J. Sun, C. Zhong, B. Li, X. You, B. Liu, Z. Liu, Analyst 137 (2012) 1837–1845.
[14] H. Tian, B. Li, J.L. Zhu, H.P. Wang, Y.R. Li, J. Xu, J.W. Wang, W. Wang, Z.H. Sun, W. S. Liu, X.G. Huang, X.H. Yan, Q. Wang, X.J. Yao, Y. Tang, Dalton Trans. 41 (2012) 2060–2065.
[15] T. Cheng, Y. Xu, S. Zhang, W. Zhu, X. Qian, L. Duan, J. Am. Chem. Soc. 130 (2008) 16160–16161.
[16] X. Liu, N. Zhang, J. Zhou, T. Chang, C. Fang, D. Shangguan, Analyst 138 (2013) 901–906.

[17] M. Li, H.Y. Lu, R.L. Liu, J.D. Chen, C.F. Chen, J. Org. Chem. 77 (2012) 3670–3673.
[18] Y. Pourghaz, P. Dongare, D.W. Thompson, Y.M. Zhao, Chem. Commun. 47 (2011) 11014–11016.
[19] Y. Hu, Q.Q. Li, H. Li, Q.N. Guo, Y.G. Lu, Z.Y. Li, Dalton Trans. 39 (2010) 11344–11352.
[20] X. Zhou, P. Li, Z. Shi, X. Tang, C. Chen, W. Liu, Inorg. Chem. 51 (2012) 9226–9231.
[21] L. Xue, C. Liu, H. Jiang, Org. Lett. 11 (2009) 1655–1658.
[22] Y.P. Li, H.R. Yang, Q. Zhao, W.C. Song, J. Han, X.H. Bu, Inorg. Chem. 51 (2012) 9642–9648.
[23] S.C. Burdette, S.J. Lippard, Coord. Chem. Rev. 216 (2001) 333–361.
[24] D.T. McQuade, A.E. Pullen, T.M. Swager, Chem. Rev. 100 (2000) 2537–2574.
[25] I. Ravikumar, P. Ghosh, Inorg. Chem. 50 (2011) 4229–4231.
[26] J.A. Drewry, P.T. Gunning, Coord. Chem. Rev. 255 (2011) 459–472.
[27] D.W. Domaille, E.L. Que, C.J. Chang, Nat. Chem. Biol. 4 (2008) 168–175.
[28] S.W. Thomas III, G.D. Joly, T.M. Swager, Chem. Rev. 107 (2007) 1339–1386.
[29] L. Basabe-Desmonts, D.N. Reinhoudt, M. Crego-Calama, Chem. Soc. Rev. 36 (2007) 993–1017.
[30] J.S. Yang, T.M. Swager, J. Am. Chem. Soc. 120 (1998) 5321–5322.
[31] T. Ishi-i, K. Murakami, Y. Imai, S. Mataka, J. Org. Chem. 71 (2006) 5752–5760.
[32] B.R. Kaafarani, T. Kondo, J. Yu, Q. Zhang, D. Dattilo, C. Risko, S.C. Jones, S. Barlow, B. Domercq, F. Amy, A. Kahn, J.L. Bredas, B. Kippelen, S.R. Marder, J. Am. Chem. Soc. 127 (2005) 16358–16359.
[33] T.H. Chang, B.R. Wu, M.Y. Chiang, S.C. Liao, C.W. Ong, H.F. Hsu, S.Y. Lin, Org. Lett. 7 (2005) 4075–4078.
[34] M. Lehmann, G. Kestemont, R.G. Aspe, C. Buess-Herman, M.H.J. Koch, M. G. Debije, J. Piris, M.P. de Haas, J.M. Warman, M.D. Watson, V. Lemaur, J. Cornil, Y.H. Geerts, R. Gearba, D.A. Ivanov, Chem. Eur. J. 11 (2005) 3349–3362.
[35] J.R. Galán-Mascarós, K.R. Dunbar, Chem. Commun. (2001) 217–218.
[36] H. Grove, J. Sletten, M. Julve, F. Lloret, J. Chem. Soc. Dalton Trans. (2001) 1029–1034.
[37] M.G. Fraser, C.A. Clark, R. Horvath, S.J. Lind, A.G. Blackman, X.Z. Sun, M. W. George, K.C. Gordon, Inorg. Chem. 50 (2011) 6093–6106.
[38] D.M. D'Alessandro, M.S. Davies, F.R. Keene, Inorg. Chem. 45 (2006) 1656–1666.
[39] S. Kitagawa, S. Masaoka, Coord. Chem. Rev. 246 (2003) 73–88.
[40] Q. Zhao, R.F. Li, S.K. Xing, X.M. Liu, T.L. Hu, X.H. Bu, Inorg. Chem. 50 (2011) 10041–10046.
[41] X.H. Zhang, Q. Zhao, X.M. Liu, T.L. Hu, J. Han, W.J. Ruan, X.H. Bu, Talanta 108 (2013) 150–156.
[42] D.Z. Rogers, J. Org. Chem. 51 (1986) 3904–3905.
[43] M.E. Hill, F. Taylor, J. Org. Chem. 25 (1960) 1037–1038.
[44] A.X.S. Bruker, SAINT Software Reference Manual Madison, WI, 1998.
[45] G.M. Sheldrick, SHELXTL NT: Program for Solution and Refinement of Crystal Structures Version 5.1 University of Göttingen: Göttingen, Germany, 1997.
[46] A.L. Spek, PLATON, Utrecht University, Utrecht, The Netherlands, 2008.
[47] C.H. Tan, S.H. Yang, N.R. Champness, X. Lin, A.J. Blake, W. Lewis, M. Schroder, Chem. Commun. 47 (2011) 4487–4489.
[48] A.L. Spek, Acta Crystallogr. Sect. D Biol. Crystallogr. 65 (2009) 148–155.
[49] W.B. Yang, A. Greenaway, X. Lin, R. Matsuda, A.J. Blake, C. Wilson, W. Lewis, P. Hubberstey, S. Kitagawa, N.R. Champness, M. Schroder, J. Am. Chem. Soc. 132 (2010) 14457–14469.
[50] (Gaussian 09, Revision B.01) M.J. Frisch, G.W. Trucks, H.B. Schlegel, G. E. Scuseria, M.A. Robb, J.R. Cheeseman, G. Scalmani, V. Barone, B. Mennucci, G.A. Petersson, H. Nakatsuji, M. Caricato, X. Li, H.P. Hratchian, A.F. Izmaylov, J. Bloino, G. Zheng, J.L. Sonnenberg, M. Hada, M. Ehara, K. Toyota, R. Fukuda, J. Hasegawa, M. Ishida, T. Nakajima, Y. Honda, O. Kitao, H. Nakai, T. Vreven, J. A. Montgomery Jr., J.E. Peralta, F. Ogliaro, M. Bearpark, J.J. Heyd, E. Brothers, K. N. Kudin, V.N. Staroverov, R. Kobayashi, J. Normand, K. Raghavachari, A. Rendell, J.C. Burant, S.S. Iyengar, J. Tomasi, M. Cossi, N. Rega, J.M. Millam, M. Klene, J.E. Knox, J.B. Cross, V. Bakken, C. Adamo, J. Jaramillo, R. Gomperts, R. E. Stratmann, O. Yazyev, A.J. Austin, R. Cammi, C. Pomelli, J.W. Ochterski, R. L. Martin, K. Morokuma, V.G. Zakrzewski, G.A. Voth, P. Salvador, J. J. Dannenberg, S. Dapprich, A.D. Daniels, O. Farkas, J.B. Foresman, J.V. Ortiz, J. Cioslowski, D.J. Fox, Gaussian, Inc., Wallingford CT, 2009.
[51] A.D. Becke, J. Chem. Phys. 98 (1993) 5648–5652.
[52] A.D. Becke, J. Chem. Phys. 98 (1993) 1372–1377.
[53] A.D. Becke, Phys. Rev. A 38 (1988) 3098–3100.
[54] C. Lee, W. Yang, R.G. Parr, Phys. Rev. B 37 (1988) 785–789.
[55] P.J. Hay, W.R. Wadt, J. Chem. Phys. 82 (1985) 299–310.
[56] J.W. Wang, J. Wu, Y.M. Chen, H.P. Wang, Y.R. Li, W.S. Liu, H. Tian, T. Zhang, J. Xu, Y. Tang, Dalton Trans. 41 (2012) 12936–12941.
[57] W.W. Huang, H. Lin, H.K. Lin, Sensor. Actuat. B 153 (2011) 404–408.
[58] Z.Y. Xiao, X. Zhao, X.K. Jiang, Z.T. Li, Chem. Mater. 23 (2011) 1505–1511.
[59] Q. Zhao, X.M. Liu, W.C. Song, X.H. Bu, Dalton Trans. 41 (2012) 6683–6688.
[60] N. Aliaga-Alcalde, L. Rodriguez, M. Ferbinteanu, P. Hofer, T. Weyhermuller, Inorg. Chem. 51 (2012) 864–873.
[61] M. Mameli, M.C. Aragoni, M. Arca, C. Caltagirone, F. Demartin, G. Farruggia, G. De Filippo, F.A. Devillanova, A. Garau, F. Isaia, V. Lippolis, S. Murgia, L. Prodi, A. Pintus, N. Zaccheroni, Chem. Eur. J. 16 (2010) 919–930.
[62] G.M. Cockrell, G. Zhang, D.G. VanDerveer, R.P. Thummel, R.D. Hancock, J. Am. Chem. Soc. 130 (2008) 1420–1430.